On the possibility of using plasmonic metal nanoparticles embedded within the silicon substrate to enhance the energy conversion efficiency of silicon thin-film solar cells

Saniat Ahmed Choudhury
Department of Electrical and Electronic Engineering
Independent University, Bangaldesh
Dhaka, Bangladesh
ac.saniat@gmail.com

Rashid Ahmed Rifat
Department of Electrical and Electronic Engineering
Independent University, Bangaldesh
Dhaka, Bangladesh
rifat308bd@gmail.com

Fatema Fairooz
Department of Electrical and Electronic Engineering
Independent University, Bangaldesh
Dhaka, Bangladesh
fatemafairooz11@gmail.com

Washaka Mahdi
Department of Electrical and Electronic Engineering
Independent University, Bangaldesh
Dhaka, Bangladesh
washakamahdi@gmail.com

Mustafa Habib Chowdhury
Department of Electrical and Electronic Engineering
Independent University, Bangaldesh
Dhaka, Bangladesh
mchowdhury@iub.edu.bd*

***Abstract*—While photovoltaic cells have become increasingly available commercially over the last few decades, their relatively low efficiencies leave much room for improvement. Plasmonic nanostructures have been used to enhance the optical and electrical activity within PV cells. However, while plasmonic nanostructures have been placed above the surface of the cell, the effect that nanostructures embedded within the cell can have on its energy conversion has not been extensively studied. This study analyzes the effect of plasmonic nanostructures embedded within a thin-film amorphous Si solar cell on the efficiency of the solar cell, and hopes to provide a relationship between the physical parameters of the nanostructures and the optical and electrical enhancement within the solar cell. The parameters considered were the size of the nanoparticles and the distance between neighboring nanoparticles. The metal chosen for the nanospheres is silver (Ag). The analyses performed were – plasmon resonance analyses, absorption enhancement, short circuit current density and near field enhancement imaging. Through this study, it was found that although there is no linear increase in optical and electrical activity with respect to particle size, the largest particle (diameter of 500nm) studied resulted in the highest enhancement. Furthermore, the closer the particles were, the greater the enhancements obtained.**

Keywords— plasmonics; solar cell; thin-film solar cell; metal nanoparticles; silver nanoparticles; nanostructures.

I. INTRODUCTION

Photovoltaics provide the most feasible alternative to non-renewable sources such as fossil fuels [1]. Considering the constantly depleting nature of the latter and its adverse contribution to climate change, it is vital that a suitable alternative be found. In order to gradually move away from fossil fuels, solar energy has to be a more viable alternative. The technology necessary to harness solar energy is solar cells or photovoltaic (PV) cells [1]–[3]. These convert solar energy to electrical energy via the generation of electron-hole pairs due to energy provided by photons in the sunlight [1]–[3]. While this should technically be an attractive alternative, the relatively low efficiencies of solar cells prevent it from being commercially viable alternatives, especially in developing countries. Because silicon is widely available and economically feasible, it is considered to be the most suitable material for the production of solar cells [3]. However, present Si based solar cells have very low efficiencies, with the highest recorded to be 25% [4], while those commercially available can barely reach 15%-18% under optimum conditions [3]-[4]. While there are several methods utilized to enhance solar cell efficiencies, including the utilization of quantum dots [5]-[6] and mesoscopic nanostructures [7]-[8], this study focuses on plasmonically enhanced solar cells [9]-[10].

The authors of this study have previously analyzed the efficacy of plasmonic nanostructures placed periodically on top of Si substrate [10]-[14]. The physical parameters of the nanostructures were altered, and a relationship between those parameters and the optical absorption and electrical current generation enhancement of the Si substrate were established [10]-[14]. It is only natural, therefore, that the next analyses be done on plasmonic nanostructures embedded within the Si substrate itself. However, previous literature search has yielded that very little research has been done in this respect [15]-[27]. Hence, this study hopes to provide the basis for a fundamental understanding of this technique through simulation-based studies. A rudimentary relationship between key physical parameters of the nanostructures and the energy conversion efficiency of the thin-film solar cells is established. The nanostructures have been chosen to be spherical in shape, and the parameters that have been analyzed are nanoparticle size and the interparticle distance. The type of plasmonic metal was

kept constant with silver (Ag), as this has been previously found to yield the best results by both early investigators and the authors as well [10]-[14], [19]-[21]. The analyses that were performed to stipulate our observations are plasmon resonance analysis, absorption enhancement analysis, short circuit current density analysis and near-field enhancement analysis.

II. Materials and Methods

A. Simulation Setup

The simulations performed were done using the solvers – (i) FDTD Solutions [28], a commercial-grade simulator that uses the finite-difference time-domain method to perform the calculations, for the optical enhancement analysis, while (ii) CHARGE (DEVICE) [29], a commercial-grade simulator eigenmode solver and propagator, was used for the electrical analysis portion, i.e. calculation of short circuit current density (J_{SC}) for all configurations. The solvers were developed by Lumerical Solutions, Inc. All of the simulations were performed under the following conditions: temperature of 25°C, incident radiation intensity of 1000 W/m^2, and a solar spectral irradiance of AM1.5G [30].

B. Procedure

Before we began our analysis, we had to first identify the physical parameters that were of interest to us. To that end, we chose silver (Ag) as the plasmonic metal that we wished to analyze. The diameters of the nanospheres we chose were D = 50nm, D = 100nm D = 200nm and D=500nm as we induced that this would provide us with a sufficient amount of data to establish an acceptable conclusion. Furthermore, we also chose four different pitches (distance between the ends of successive or neighboring particles) to be P=10nm, P=20nm, P=50nm and P=100nm.

The entire analysis can be broken down into four major sections: (a) plasmonic resonance analysis of individual nanoparticles, (b) absorption enhancement analysis of the PV cell, (c) short circuit current density (J_{SC}) analysis, and (d) near field enhancement analysis

Our first task was to observe and analyze the plasmonic resonance phenomenon of each metal nanoparticle inside the Si substrate, and identify the wavelength range where the resonance of each nanoparticle occurred. Thus, we chose to calculate the extinction, scattering and absorption spectra of incident radiation for each nanoparticle. To this end, we placed the metal nanoparticle of interest in our simulation region, and directed a total field scattered field (TFSF) source towards it from all directions. Field monitors were placed close to the particle to measure absorption, and outside the particle beyond the source to measure scattering. The extinction spectrum was generated by adding these two quantities.

We then placed a horizontal array of each metal nanoparticle periodically inside (0.5µm below the surface) of a 2µm thick Si substrate, and then directed a plane wave orthogonally towards the PV cell. Field monitors were placed right at the metal nanoparticle array and Si interface, and 0.5µm perpendicularly below the nanoparticle array. The

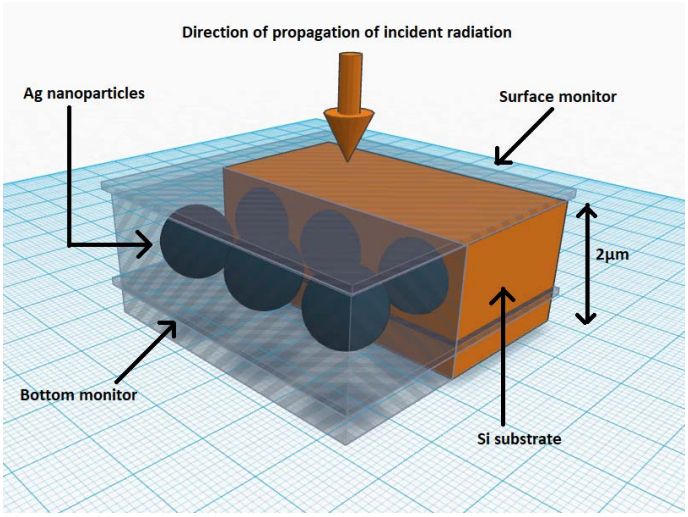

Figure 1. Absorption enhancement analysis setup.

absorption within the cell was calculated by subtracting the output values of the upper monitor from the lower monitor. The setup has been shown in Figure 1. For each metal nanoparticle array, we needed to analyze the optical enhancement within the Si substrate for each array. To that end, we identified the quantity absorption enhancement factor (g) as the most appropriate. This was calculated using the following formula:

$$g = \frac{Absorption\ across\ Si\ with\ metal\ nanoparticles}{Absorption\ across\ bare\ Si} \qquad (1)$$

In order to keep variations from other factors in check and calculate the enhancement with respect to just one parameter, we kept the other parameters constant, e.g. if we wanted to measure the enhancement due to a metal nanoparticle of diameter D = 50nm, we kept the diameter constant at 50 nm, and only varied the pitch size.

The electrical enhancement was then calculated by the short circuit current density (J_{SC}) for each configuration of Ag nanoparticle array inside the substrate, and compared with the J_{SC} of a bare Si substrate.

Finally, the interaction of the electromagnetic fields within the PV cells was analyzed by generating near-field images of each of our respective metal nanoparticle structures. This was achieved by placing a field monitor along the vertical cross-section of three units of the cell, i.e. the section of the Si substrate with three Ag nanoparticles inside. The near field images would allow us to properly link the optical and electrical enhancements with the enhancement in the electromagnetic fields with the PV cell due to the presence of the metal nanoparticle array. It would also show us how the nanoparticles interact with each other within the substrate.

III. Results and Discussions

The results and discussions have been divided into separate sections for each respective analysis.

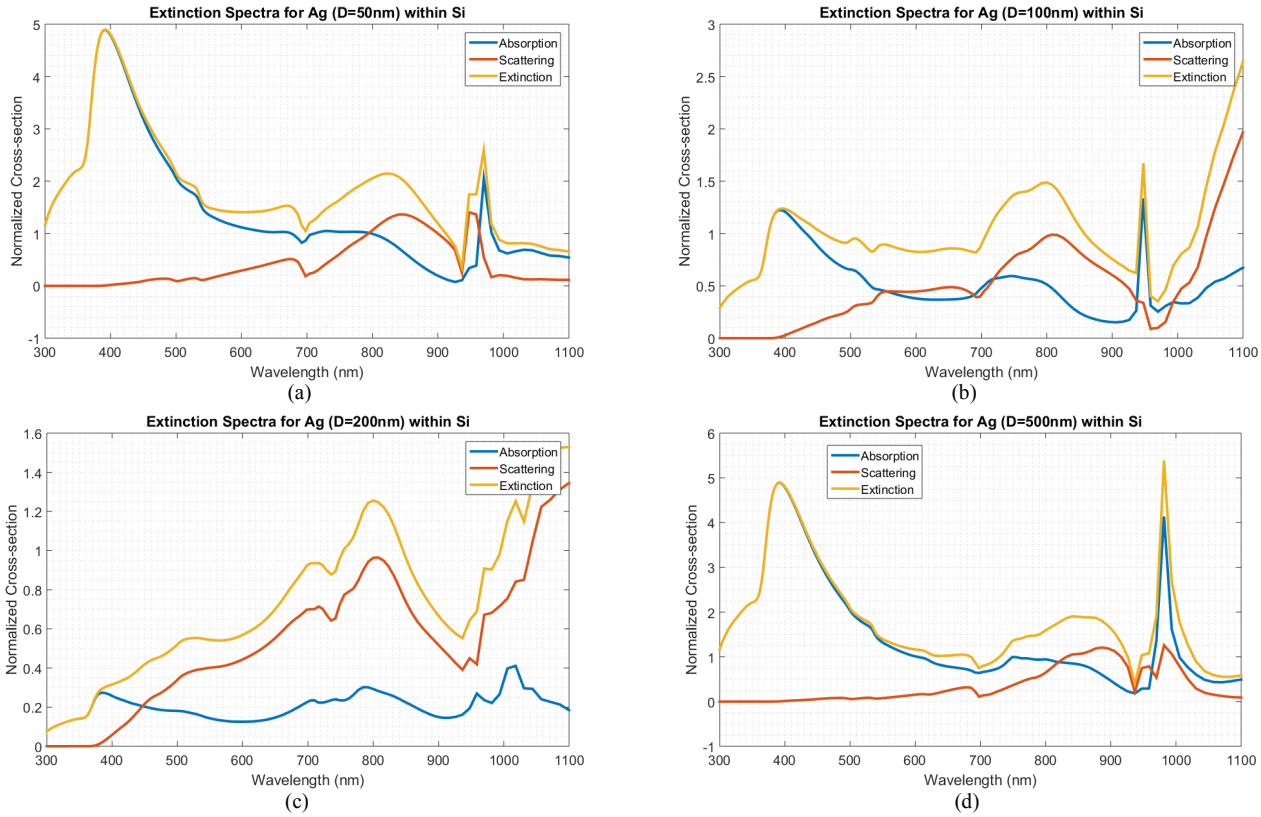

Figure 2. Absorption, scattering and extinction spectra for (a) Ag nanoparticle of D = 50nm, (b) Ag nanoparticle of D = 100nm (c) Ag nanoparticle of D = 200nm, (d) Ag nanoparticle of D = 500nm.

A. Plasmon Resonance

For the initial simulation, we analyzed the extinction spectra of Ag plasmonic metal nanoparticles of diameters D = 50nm, D = 100nm, D = 200nm and D=500nm, respectively. The particles were separately and individually placed inside the Si substrate, and this entire structure was then placed in the simulation region. The absorption, scattering and extinction spectra were then obtained using the appropriately placed monitors. The resultant spectra from the simulations are shown in Figures 2(a) through (d).

The analysis was done across a wide wavelength range of λ = 400nm to 1100nm as Ag nanoparticles have been known to demonstrate plasmon resonance in this region. For all four particles analyzed, it can be seen that there are multiple resonance peaks that occur at relatively similar wavelengths. The most pronounced peak is found to be around 810nm for each nanoparticle, while the second sharp peak shifts for each particle – approx. 950nm, 980nm, 1000nm and 1010nm for D=50nm, D=100nm, D=200nm and D=500nm, respectively. The results will be fundamentally different because Si is highly dispersive (and absorbing) material in this frequency range. This poses a challenge because the Si may in fact be absorbing and/or otherwise modifying the incident radiation. This can be one reason behind the formation of multiple resonance peaks as shown in Figures 2(a-d).

B. Absorption Enhancement Analysis

For the absorption enhancement analysis, the simulation was setup as previously shown in Figure 1. The metal is kept constant (Ag) while the diameter of the nanoparticles periodically dispersed at a constant end-end pitch of 10nm inside the Si substrate are varied, and the absorption enhancement factor (g) for each configuration is calculated across their respective incident radiation spectra. This is repeated for all four sizes of nanoparticles. The pitch (end-end) is then changed to 20nm, 50nm and 100nm, respectively, and the above analysis is repeated for each Ag nanoparticle size. The absorption enhancement analysis for Ag nanoparticles embedded within the Si substrate for all sizes and pitches are shown in Figure 3. Once again, the graphs show multiple absorption peaks due to the dispersive and absorbing nature of the Si substrate that the Ag nanoparticles are embedded in. Because of this property, it is possible that the reflected radiation from the Ag-Si interface interfered with the original incident radiation and/or with each other, resulting in the oscillating pattern that can be seen. It is noticeable that the configurations with nanoparticle diameter of D=500nm demonstrates relatively the highest absorption enhancement when compared with the other configurations studied.

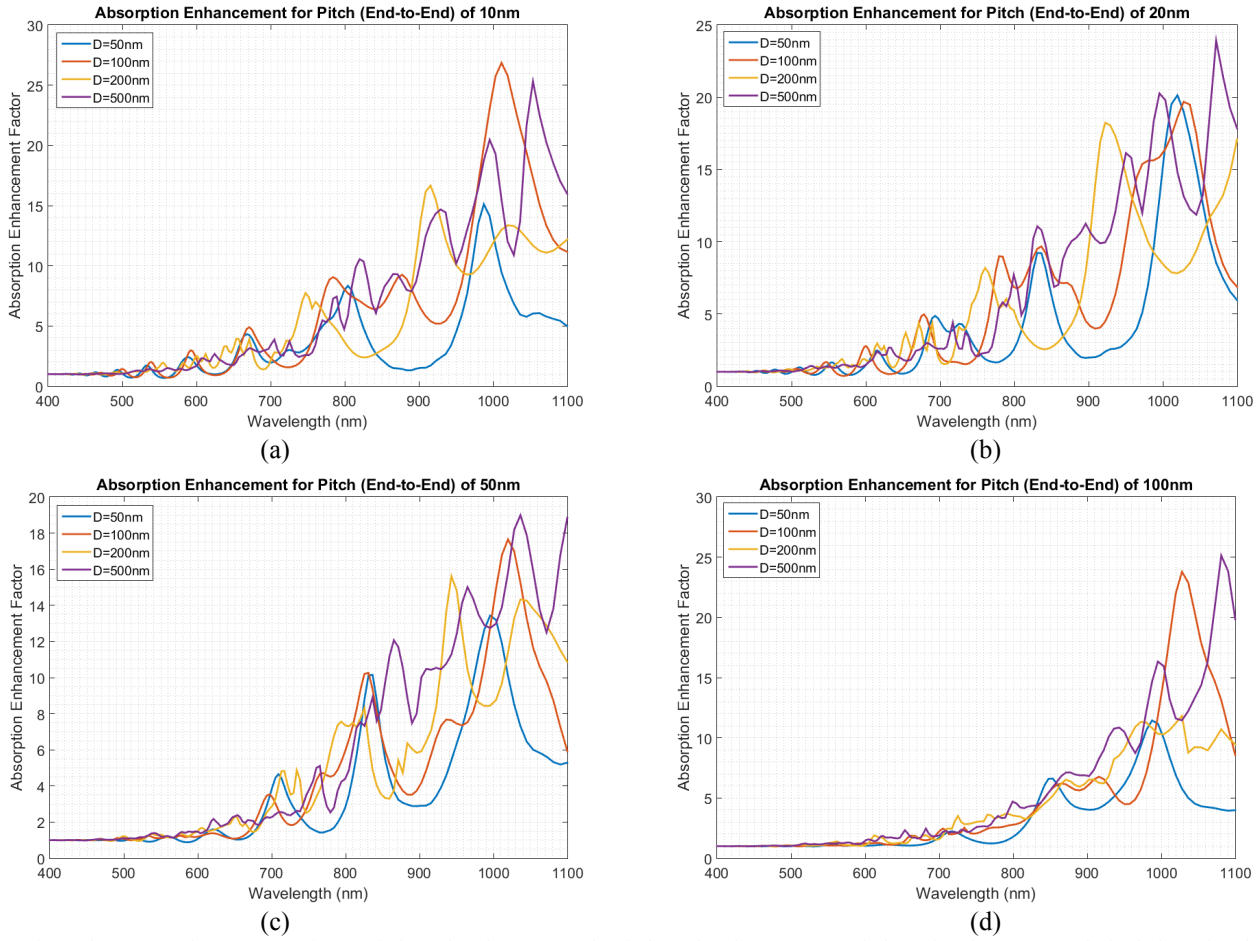

Figure 3. Absorption enhancement factor spectra for (a) pitch (end-end) = 10nm, (b) pitch (end-end) =20nm, (c) pitch (end-end) =50nm, and (d) pitch (end-end) =100nm.

In order to further understand these results, the total absorption enhancement for the entire spectrum of each configuration is calculated and the results are shown in Figure 4. A general pattern for all pitches arises from this graph – the D=50nm nanoparticle shows the least total enhancement, and then it increases for D=100nm, decrease for D=200nm and then shows the highest total enhancement for D=500nm. Additionally, the general trend of the data in Figure 4 show the highest set of absorption enhancements for the smallest end-end pitch, i.e. P=10nm. This is because the nanoparticles are closest together for this small pitch size, and are thus able to better plasmonically couple with each other and also with the incident and/or any scattered radiation.

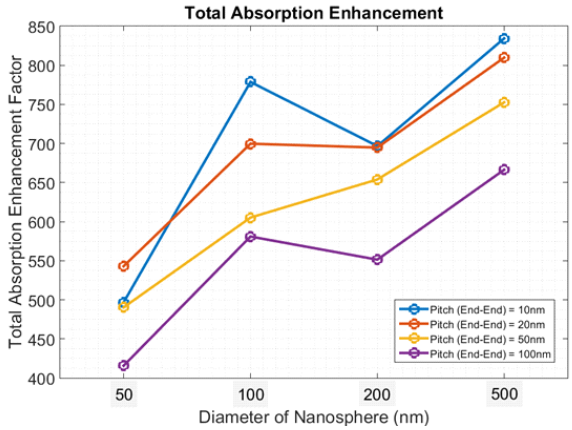

Figure 4. Total optical absorption enhancement for different configurations.

C. *Short Circuit Current Density Analysis*

It can be expected that the increase in optical absorption within the Si substrate as shown can result in a proportional increase in electrical activity [10]-[14]. However, in real conditions, this is not strictly so, as electricity generation depends on a number of factors, including minority carrier lifetime and carrier recombination rate. Thus, to coherently identify the extent to which the increase in optical absorption enhancement of the Si substrate due to the presence of the metal nanoparticles has translated in terms of electricity generation of the cell, the short circuit current density (J_{SC}) of the cell was calculated for each respective configuration. The results have been graphically illustrated in Figure 5. The general trend in J_{SC} observed is very similar to that of total absorption enhancement of Figure 4. Furthermore, the highest J_{SC} is found to be for the smallest pitch (inter-particle distance). The increase in the amount of J_{SC} generation is found to be significantly greater to that of previous studies where plasmonic nanostructures were placed on top of the Si substrate [10]-[14].

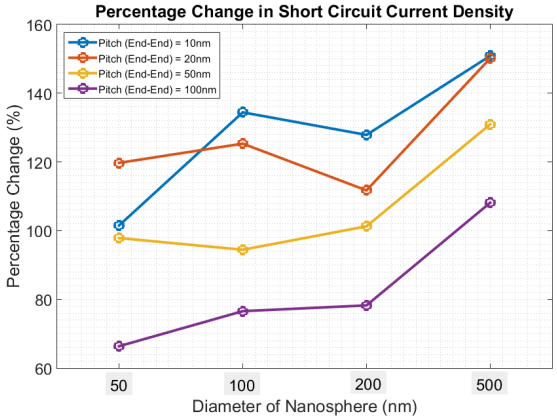

Figure 5. Percentage change in J_{SC} for different configurations.

D. Near-Field Enhancement Analysis

Near-field images would help elucidate the relationship between transmission of the electric field within/around the nanoparticle and the Si substrate at the resonant wavelength of the particle, and the improved optical and electrical enhancement that we have shown earlier. It would also show the extent of plasmonic coupling that occurs between the metal nanoparticles. To this end, we generated near-field plots for Ag nanoparticle arrays of different size and pitches in order to be able to properly compare and contrast the electromagnetic interactions within the structures themselves. This will enable us to build a more comprehensive link between the variation of the physical parameters of the Ag nanoparticle (arrays) and the improvement in electrical activity. First, we had to identify the approximate wavelength at which the nanoparticles of all diameters displayed surface plasmon resonance. This was found to be wavelengths of approximately $\lambda \sim 810$nm for all nanoparticles. Three near-field images were generated for each respective nanoparticle configuration – (a) the Si substrate without the particle at the given wavelength (b) the Si substrate with three of the respective metal nanoparticle particles (embedded) at the given wavelength and; (c) the enhancement image, which was calculated by dividing the raw data of the second image (calculated in (b)) with the raw data of the first image (calculated in (a)). For the enhancement image, the color scale is in the log scale, and hence the areas which are dark red in color have an enhancement of over 1 in the log scale that corresponds to near-field enhancement of over ×10 (over 10 fold). A selected set of near-field enhancement images are provided in Figure 6. For these images, the near-field monitor has been placed inside the Si, with only the Si substrate and the nanoparticles within its region of analysis.

The enhancement within the substrate can be observed clearly, and for smaller pitches (Figures 6(a) and 6(b)) it is seen that the enhancements from each nanoparticle is spread across neighboring particles, which can be indicative of strong plasmonic coupling between neighboring metal nanoparticles. There is a significant amount of enhancement noticeable both above and below the particle. The enhancement above is high. This can be attributed to the fact that radiation is constantly being reflected back and forth between the Si-air interface and the top portion of the Ag-Si interface, forming a cavity like phenomenon that intensifies the electromagnetic fields due to constant constructive interference. This may in turn result in enhanced optical absorption within the substrate, and explain

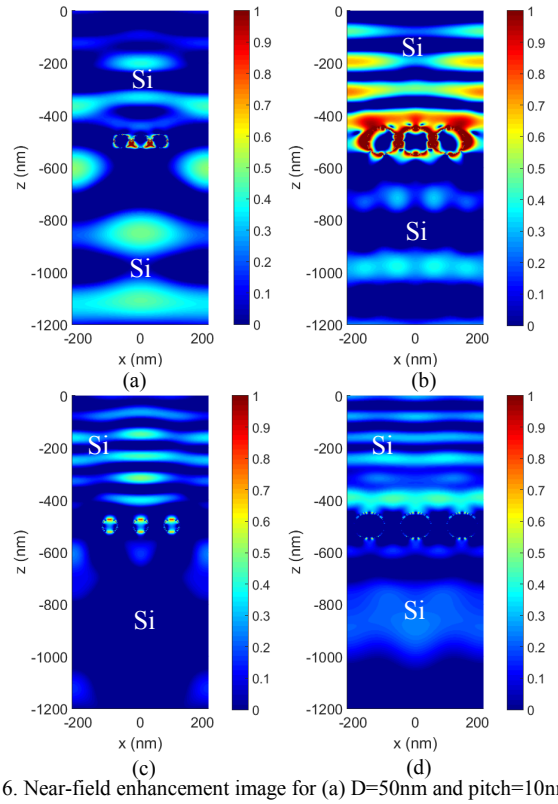

Figure 6. Near-field enhancement image for (a) D=50nm and pitch=10nm, (b) D=100nm and pitch=10nm, (c) D=50nm and pitch=20nm, and (d) D=100nm and pitch =20nm. The images generated are focused within the Si substrate.

the observations made in absorption enhancement and short circuit current density portions of the analysis.

IV. Conclusion

An attempt at generating a fundamental simulation-based understanding of the relationship between key physical parameters of Ag nanoparticles embedded within an amorphous thin-film Si substrate and the optical and electrical enhancement generated from the same substrate has been made in this study. The parameters studied were the size of the nanoparticles and the end-end pitch of the nanoparticle array placed inside the substrate. Through multiple stages of analysis it was found that the largest particle size studies (D=500nm) resulted in the highest optical enhancement within the substrate. Furthermore, it was also found that the closer the particles were to each other, the greater the amount of enhancement it resulted in. A study of the short circuit current density generated by each configuration showed that the trend in optical enhancement was similar to that of the electrical current enhancement. It is also shown that decreasing the pitch size leads to a larger increase in the J_{SC}. Significant increases in the J_{SC} by as much as 150% can be observed, which makes this configuration of plasmonic solar cells amenable to further analysis. This has been further verified by analyzing near-field enhancement images which not only demonstrated the enhancement in electromagnetic intensity due to the presence of the metal nanoparticles, but also supported the claims of the above aforementioned conclusion. The images also showed that a larger amount of enhancement occurs above the nanoparticle array than below it, possibly due to constructive interference of radiation reflected from interfaces and the incident radiation. This has allowed the authors to conclude

that the size of the nanoparticles and their pitches have a significant influence over their capability to enhance the optical and electrical activity within the substrate in which it is embedded.

Of course, further analysis is necessary to establish a more robust understanding of these relationships. Other electrical parameters such as open circuit voltage (V_{OC}), peak power, fill factor and efficiency must also be analyzed to obtain a better understanding of solar cell efficiency. Future work in this field shall include the calculations and analysis of these additional parameters, and the mathematical modeling of the complexities of the shapes of the metal nanoparticles to explain more exhaustively the reasons for which the largest metal nanoparticle with the smallest pitch is showing better results than the other configurations studied. It appears there is an interesting scope to design/simulate plasmonic solar cells with metal nanoparticle arrays placed both on top of the Si substrate and also embedded within the Si substrate to obtain very high levels of optical absorption enhancement and also short circuit current generation. In such applications, further work must be done to understand the effects of having the plasmonic metal nanoparticles embedded within a dispersive and absorbing media such as Si.

ACKNOWLEDGMENT

The authors would like to thank Independent University, Bangladesh (IUB) for funding the research and Dr. M. Abdur Razzak for his endless support and encouragement and also for securing funding for this research.

REFERENCES

[1] U. Eicker, E. Demir and D. Gürlich, “Strategies for cost efficient refurbishment and solar energy integration in European Case Study buildings,” Energy and Buildings, vol. 102, pp. 237-249, 2015.

[2] J. Nelson, The Physics of Solar Cells. London, England: Imperial College Press, 2003.

[3] P. Wüffel, Physics of Solar Cells: Principles to New Concepts. New York, NY: Wiley-VCH, 2004.

[4] K. Masuko, M. Shigematsu and T. Hashiguchi, “Achievement of more than 25% conversion efficiency with crystalline silicon heterojunction solar cell,” IEEE Journal of Photovoltaics, vol. 4 (6), 2014.

[5] X. Lan, O. Voznyy, A. Kiani et al., “Passivation Using Molecular Halides Increases Quantum Dot Solar Cell Performance,” Adv. Mat., vol. 28 (2), pp. 299-304, 2016.

[6] X. lan, O. Voznyy, F. P. Arquer et al., “10.6% Certified Colloidal Quantum Dot Solar Cells via Solvent-Polarity-Engineered Halide Passivation,” Nano Lett., vol. 16 (7), pp. 4630-4634, 2016.

[7] S. Jang, J. S. Kang, J. Lee et al., “Light Harvesting: Enhanced Light Harvesting in Mesoscopic Solar Cells by Multilevel Multiscale Patterned Photoelectrodes with Superpositioned Optical Properties,” Adv. Func. Mat., vol. 26 (36), pp. 6583, 2016.

[8] X. Li, W. C. H. Choy, H. Lu, W. E. I. Sha, and A. H. P. Ho, “Efficiency Enhancement of Organic Solar Cells by Using Shape-Dependent Broadband Plasmonic Absorption in Metallic Nanoparticles,” Adv. Func. Mat., vol. 23 (21), pp. 2728-2735, 2013.

[9] P. Reineck, D. Brick, P. Mulvaney, and U. Bach, “Plasmonic Hot Electron Solar Cells: The Effect of Nanoparticle Size on Quantum Efficiency,” J. Phys. Chem. Lett., 2016.

[10] S. A. Choudhury, M. S. Munir, N. Nawshin and M. H. Chowdhury, “Effect of varying the row and column size of periodic arrays of plasmonic nanoparticles on the energy conversion efficiency of thin-film solar cells,” International Conference on Electrical, Computer and Communication Engineering (ECCE), pp. 44 – 49, 2017.

[11] S. A. Choudhury and M. H. Chowdhury, “Use of plasmonic metal nanoparticles to increase the light absorption efficiency of thin-film solar cells,” IEEE 4th International Conference on Sustainable Energy Technologies, Hanoi, Vietnam, 2016.

[12] S. A. Choudhury and M. H. Chowdhury, “Optimizing the Parameters of Plasmonic Metal Nanoparticles to Maximize the Energy Conversion Efficiency of Thin-Film Solar Cells,” 3rd International Conference on Electrical Engineering and Information and Communication Technology, MIST, Dhaka, Bangladesh, 2016.

[13] S. A. Choudhury and M. H. Chowdhury. “The Promise and Challenges of Enhancing Solar Cell Efficiency Using Patterned Nanostructures,” 1st International Conference on Advanced Information and Communication Technology, Chittagong, Bangladesh, 2016.

[14] T. Repäna, S. Pikkera, L. Dolgova, A. Loota, J. Hiieb, M. Krunksb, I. Sildosa, “Increased efficiency inside the CdTe solar cell absorber caused by plasmonic metal nanoparticles,” Energy Procedia, vol. 44, pp. 229233, 2014.

[15] L. Liu, G. D. Barber, M. V. Shuba, Y. Yuwen, A. Lakhtakia, T. E. Mallouk, and T. S. Mayer, “Planar Light Concentration in Micro-Si Solar Cells Enabled by a Metallic Grating–Photonic Crystal Architecture,” ACS Photonics, 2016, vol. 3 (4), pp 604–610, 2016.

[16] N. P. Hylton, X. F. Li, V. Giannini, K. -H. Lee, N. J. Ekins-Daukes, J. Loo, D. Vercruysse, P. Van Dorpe, H. Sodabanlu, M. Sugiyama, and S. A. Maier, “Loss mitigation in plasmonic solar cells: aluminium nanoparticles for broadband photocurrent enhancements in GaAs photodiodes,” Scientific Reports, vol. 3, art. 2874, 2013.

[17] S. Lombardo, A. Battaglia, M. Foti, C. Tringali, G. Cannella, N. Costa c, C. Gerardi, F. Principato, “Plasmonic Modes in Molybdenum Ultra-thin Films Suitable for Hydrogenated Amorphous Silicon Thin Film Solar Cells,” Energy Procedia, vol. 44, pp. 216-222, 2014.

[18] W. Raja1, A. Bozzola, P. Zilio, E. Miele, and S. Panaro, “Broadband absorption enhancement in plasmonic nanoshells-based ultrathin microcrystalline-Si solar cells,” Scientific Reports, vol. 6, 2016.

[19] M. S. U. I. Sami, R. Rahman, F. Pervin and F. M. Mohammedy, "Efficiency enhancement and reflectance reduction of thin film silicon plasmonic solar cells," IEEE 6th International Conference on Photonics (ICP), Kuching, pp. 1-3, 2016.

[20] Y. Rong, X. Hou, Y. Hu et al., “Synergy of ammonium chloride and moisture on perovskite crystallization for efficient printable mesoscopic solar cells,” Nat. Commun., vol. 8, 2017.

[21] F. Dimroth, M. Grave et al., “Wafer bonded four-junction GaInP/GaAs//GaInAsP/GaInAs concentrator solar cells with 44.7% efficiency,” Progress In Photovoltaics, vol. 22 (3), pp. 277-282, 2014.

[22] J. He, Z. Yang et al., “Enhanced Electro-Optical Properties of Nanocone/Nanopillar Dual-Structured Arrays for Ultrathin Silicon/Organic Hybrid Solar Cell Applications,” Advanced Energy Materials, vol. 6 (8), 2016.

[23] S. Yuna, Y. H. Paikb, S. J. Kimb, D. G. Kimc, T. Jia and J. C. Shin, “High efficiency AZO-InP nanopillar-based heterojunction solar cells,” Current App. Physics, vol. 16 (7), pp. 726-730, 2016.

[24] H. Kwon, A. Kim, H. Lee, D. Lee. S. Jeong and J. Moon, “Parallelized Nanopillar Perovskites for Semitransparent Solar Cells Using an Anodized Aluminum Oxide Scaffold,” Adv. En. Mat., vol. 6 (20), 2016.

[25] J. Hie, Z. Yang, P. Liu et al., “Hybrid Solar Cells: Enhanced Electro-Optical Properties of Nanocone/Nanopillar Dual-Structured Arrays for Ultrathin Silicon/Organic Hybrid Solar Cell Applications,” Adv. En. Mat., vol. 6 (8), 2016.

[26] P Jain, P Shokeen, and P Arun, “Improved efficiency of plasmonic tin sulfide solar cells,” Journal of Mat. Sc.: Mats. In Elec., vol. 27 (5), pp. 5107-5113, 2016.

[27] Lumerical Solutions, Inc. http://www.lumerical.com/tcad-products/fdtd/.

[28] Lumerical Solutions, Inc. http://www.lumerical.com/tcadproducts/device/.

[29] C. F. Bohren, and D. R. Huffman, Absorption and Scattering of Light by Small Particles. New Work, NY: Wiley, 1983.